Heterahelicenes: Diazadithia[7]helicenes were synthesized from the readily available building block ethyl 7-chloro-8-formylthieno[3,2-*f*]quinoline-2-carboxylate by a Wittig reaction–photocyclization strategy. The helicene core was functionalized by nucleophilic aromatic substitution with a variety of nucleophiles, Suzuki coupling, and Buchwald–Hartwig amination. Racemization studies confirmed that the enantiopure forms of these [7]helicenes (see figure) are conformationally more stable than their lower analogues.

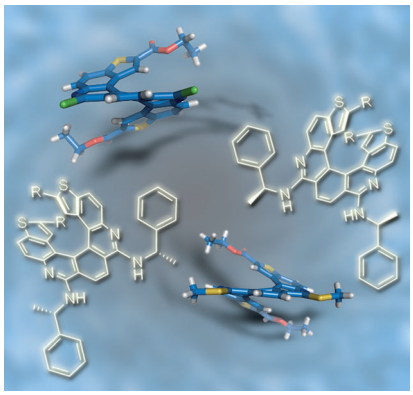

Helicenes

*D. Waghray, A. Cloet, K. Van Hecke, S. F. L. Mertens, S. De Feyter, L. Van Meervelt, M. Van der Auweraer, W. Dehaen** ..... ▮▮▮▮–▮▮▮▮

Diazadithia[7]helicenes: Synthetic Exploration, Solid-State Structure, and Properties

CHEMISTRY
A EUROPEAN JOURNAL

ChemPubSoc
Europe

DOI: 10.1002/chem.201300843

Diazadithia[7]helicenes: Synthetic Exploration, Solid-State Structure, and Properties

Deepali Waghray,[a] Arvid Cloet,[b] Kristof Van Hecke,[c] Stijn F. L. Mertens,[b] Steven De Feyter,[b] Luc Van Meervelt,[d] Mark Van der Auweraer,[b] and Wim Dehaen*[a]

Abstract: Diazadithia[7]helicenes were synthesized from the readily available building block ethyl 7-chloro-8-formylthieno[3,2-*f*]quinoline-2-carboxylate by a Wittig reaction–photocyclization strategy. The helicene core was functionalized by nucleophilic aromatic substitution with a variety of nucleophiles (e.g., O-, N-, and C-centered) and palladium-catalyzed reactions such as Suzuki coupling and Buchwald–Hartwig amination. Racemization studies confirmed that the enantiopure forms of these [7]helicenes are conformationally stable compared to their lower analogues. The solid-state structures of the novel diazadithia[7]helicenes were determined by single-crystal X-ray diffraction. The crystal structures of these azathia[7]helicenes show columnar stacking in antiparallel fashion. The HOMO–LUMO gaps of the new compounds were determined on the basis of electrochemical and optical measurements.

Keywords: chiral resolution · cyclization · helical structures · helicenes · Wittig reactions

Introduction

Heterahelicenes are a special type of condensed aromatic molecules, as they consist of *ortho*-annulated aromatic or heteroaromatic rings which arrange in a non-planar manner due to steric strain of the terminal rings, and thus give rise to helical chirality.[1] Helicenes are an interesting class of conjugated molecules currently being investigated for optoelectronic application.[2] These inherently chiral molecules combine both electronic and chiroptical properties, which can be attributed to their extended π-conjugated system and their peculiar helixlike structure. The synthesis of regiodefined heterahelicenes is of significant interest. The presence, nature, and position of heteroatoms can tune helicity parameters such as dihedral angles and bond lengths that modify the configurational stability (e.g., racemization barriers), and are thus relevant to potential applications of these compounds in materials science. Over the past years, helicenes have been extensively studied due to their self-assembly in the solid state, their ability to behave as organic conductors, and their use in optical resolution and molecular and biomolecular recognition.[3]

Aza- and thiahelicenes are a subgroup of heterahelicenes. Although an overview of the literature over the last decade highlighted carbohelicenes[4] as dominant helical frameworks, heterahelicenes[5] such as oxa-, aza-, and thiahelicenes recently emerged as an extremely attractive class of compounds. The presence of sulfur atoms has been shown to enhance the electronic and optical properties of thiahelicene-based materials. On the other hand, starting from a helicene backbone having more than one nitrogen atom, interesting supramolecular complexes can be formed. These compounds show a tendency toward π–π* stacking and building of columnar systems, which can form the basis for optoelectronic applications.[6] Azahelicene derivatives have been reported to have potential applications in the field of asymmetric catalysis, self-assembly, and metal coordination complexes,[7] whereas thiahelicenes are appealing candidates for chiral NLO materials, chiral catalysts, and asymmetric inducers and have been used as building blocks for helical conjugated polymers.[8] Combining the features of aza- and thiahelicenes would be an interesting aspect to study. We envisage that these bifunctional analogues comprising π-rich thiophene and π-deficient pyridine units would be potentially more valuable. The presence of terminal thiophene units could lead to regioselective α-functionalization of the ring system. Pyridine nitrogen atoms in the chiral helicenes can serve as hydrogen acceptors and metal chelating agents for

[a] D. Waghray, Prof. Dr. W. Dehaen
Molecular Design and Synthesis
Department of Chemistry, KU Leuven
Celestijnenlaan 200F, 3001 Leuven (Belgium)
Fax: (+32) 16327990
E-mail: wim.dehaen@chem.kuleuven.be

[b] A. Cloet, Dr. S. F. L. Mertens, Prof. Dr. S. De Feyter, Prof. Dr. M. Van der Auweraer
Molecular Imaging and Photonics
Department of Chemistry, KU Leuven
Celestijnenlaan 200F, 3001 Leuven (Belgium)

[c] Prof. Dr. K. Van Hecke
Department of Inorganic and Physical Chemistry, Universiteit Gent
Krijgslaan 281-S3, 9000 Gent (Belgium)

[d] Prof. Dr. L. Van Meervelt
Biomolecular Architecture, Department of Chemistry
KU Leuven, Celestijnenlaan 200F, 3001 Leuven (Belgium)

Supporting information for this article is available on the WWW under http://dx.doi.org/10.1002/chem.201300843.

chirality recognition. In the past few years, various methods have been described for the synthesis of azathiahelicenes, which include the classical photochemical procedure by Caronna et al.[5a,b] and a versatile synthetic method based on Bu_3SnH-mediated coupling developed by Harrowven and co-workers.[9] Furthermore, the [2+2+2] cycloisomerization of triynes[10] and palladium-catalyzed arylation[11] are among the few reported approaches to helicenes by metal-catalyzed cyclization.

An overview of past and current work is shown in Scheme 1. In our previous work,[12] we synthesized diversely functionalized diaza[5]helicenes from a readily available

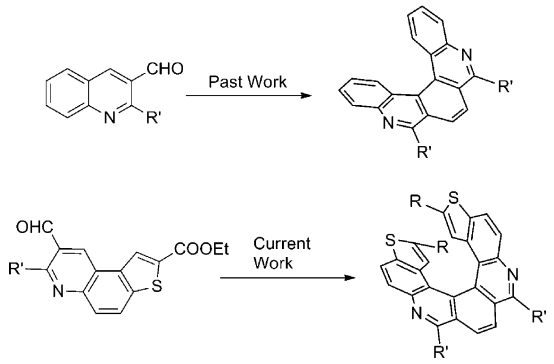

Scheme 1. Overview of past and current work.

quinoline building block by Wittig reaction and photochemical cyclization. A resolution strategy based on diastereomeric separation was developed by substituting the dichloro azahelicene derivatives with a chiral amine. In the present work we have extended the above methodology to the synthesis of diazadithia[7]helicenes from the readily available building block ethyl 7-chloro-8-formylthieno[3,2-*f*]quinoline-2-carboxylate, which was converted by a Wittig reaction–photocyclization strategy to [7]helicenes. Enantiopure forms of these [7]helicenes were conformationally very stable and had a much higher racemization barrier than the previously synthesized diaza[5]helicenes. Determination of the racemization barrier reflecting the repulsive interaction between the terminal aromatic rings is a crucial helicity indicator. Furthermore, as a proof of concept the helicene skeleton was substituted by O-, S-, N-, and C-centered nucleophiles in nucleophilic aromatic substitution reactions and palladium-catalyzed reactions such as Suzuki coupling and Buchwald–Hartwig amination.[13]

Results and Discussion

Our approach makes use of the building block ethyl 7-chloro-8-formylthieno[3,2-*f*]quinoline-2-carboxylate (**1**), which was readily prepared from ethyl 5-acetamidobenzo[*b*]thiophene-2-carboxylate by Vilsmeier chloroformylation with DMF and $POCl_3$ at 80 °C for 15 h.[14] Quinoline building block **1** was obtained in 87% yield. Ethyl 5-acetamidobenzo[*b*]thiophene-2-carboxylate was in turn prepared from ethyl 5-aminobenzo[*b*]thiophene-2-carboxylate according to literature procedures.[15] Quinoline building block **1** was converted to ethyl 8-formyl-7-(methylthio)thieno[3,2-*f*]quinoline-2-carboxylate (**2**) by reaction with NaSMe in DMF at room temperature for 2 h in 78% yield. Aldehydes **1** and **2** were converted to their corresponding alcohols **3a** and **4a** by reduction with $NaBH_4$ in THF/MeOH in 85 and 92% yield, respectively. These alcohols were converted to bromo derivatives **3b** and **4b** by reaction with PBr_3 at 0 °C in THF, which were subsequently converted to their respective phosphonium salts **3c** and **4c** by reaction with triphenylphosphine in refluxing toluene for 12–15 h in 86 and 89% yield, respectively (Scheme 2).

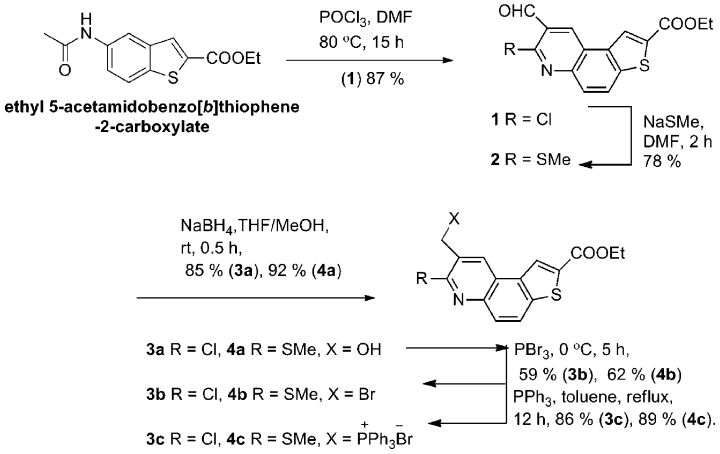

Scheme 2. Synthesis of alcohols and corresponding phosphonium salts.

Wittig olefination of **1** and **2** with phosphonium salts **3c** and **4c**, respectively, sodium *tert*-butoxide as base and THF as solvent at 0 °C for 3 h gave the corresponding symmetric azathiastilbene derivatives **5a** and **5c** in 58 and 74% yield. Similarly the reaction of aldehyde **1** with phosphonium salt **4c** gave the asymmetric azathiastilbene derivative in 69% yield (Scheme 3).

Alkenes **5a–c** were obtained with a relatively high degree of *Z* selectivity, but solubility was still very low in a variety of solvents. The *ortho* effect was evident only in the case of halo substituents on the aldehyde to control the stereochemical outcome of the Wittig reaction,[9] The SMe groups play a very small role in the cooperative *ortho* effect which operates in the course of the Wittig olefination. Due to low solubility of alkenes **5a–c**, complete spectroscopic characterization was not possible. Therefore, these compounds were characterized by HRMS. The bis(thienoquinolyl)ethene derivatives **5a–c** were subjected to oxidative photocyclization[12] with iodine as oxidant and toluene as solvent (1.0 mM). Irradiation of the reaction mixture in a photochemical reactor ($\lambda = 350$ nm) furnished diazadithia[7]helicenes **6a–c** in good yields. These helicenes showed good solubility in a variety of medium-polarity solvents and were completely characterized by NMR spectroscopy and HRMS.

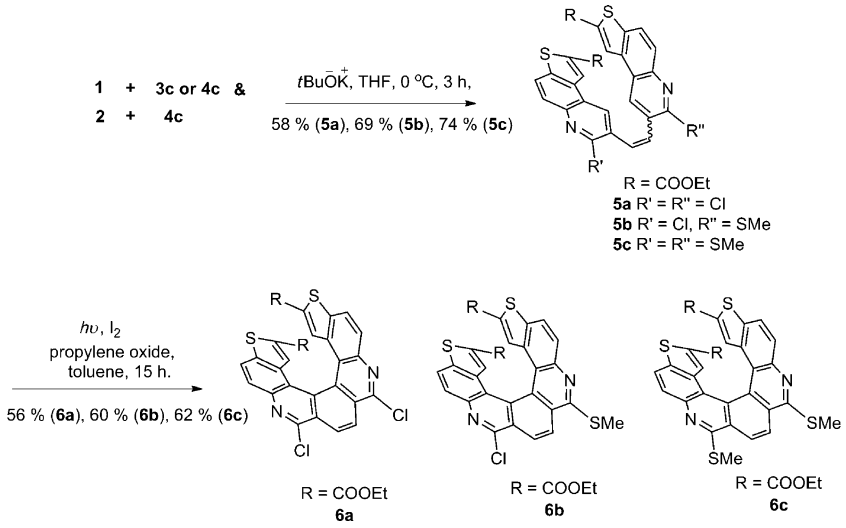

Scheme 3. Synthesis of bis(thienoquinolyl)ethene derivatives and helicenes **6a**–**c**.

Solid-state structure elucidation: Crystals of **6a** were obtained from $CHCl_3$/pentane by slow evaporation. Compound **6a** crystallized in the non-centrosymmetric orthorhombic space group $Pca2_1$; the asymmetric unit consists of two azathia[7]helicene molecules (Figure 1; for atom labeling, see Supporting Information). These two molecules are the same enantiomer, but differ from each other mainly in the spatial arrangement of their ethoxyl groups. However, in the complete crystal structure, both enantiomers are present, similar to the previously reported structure of a 5-aza[5]helicene.[5b] The distortion of the molecules, defined by the sum of the three dihedral angles C6-C11-C14-C18, C11-C14-C18-C21, C14-C18-C21-C25, and C36-C41-C44-C48, C41-C44-C48-C51, C44-C48-C51-C55 for the two azathia[7]helicene molecules, is significantly higher (77.6 and 73.6°, respectively) in comparison with 5,10-diaza[5]-helicene[16] or functionalized 6,9-dichloro- and 6,9-dimethoxy-5,10-diaza[5]helicenes.[12] In the crystal packing, the azathia[7]helicene molecules are stacked into columns along the [010] direction in an antiparallel fashion, with involvement of the outer thiophene and benzene rings (Figure 2). Several intermolecular π–π interactions are observed, in particular benzene–thiophene and benzene–benzene stacking interactions.

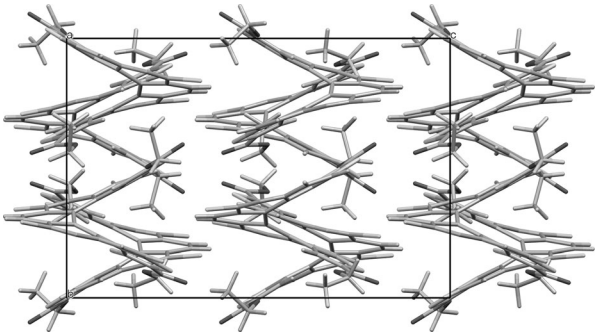

Figure 2. Packing in the crystal structure of compound **6a** along the [100] direction, showing the columnar, antiparallel stacking involving the outer thiophene and benzene rings. H atoms are omitted for clarity.

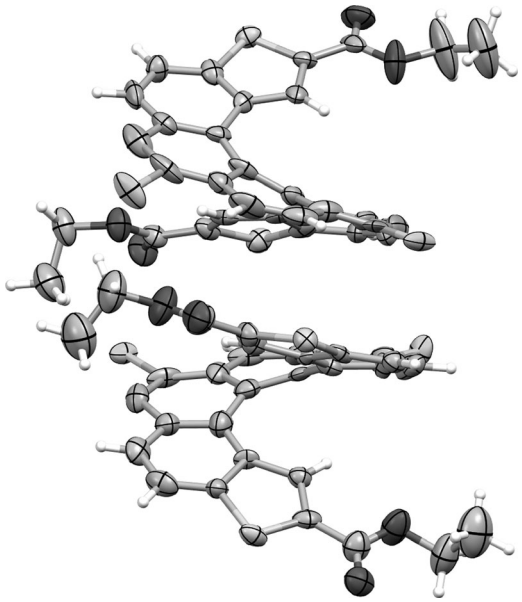

Figure 1. Asymmetric unit of the crystal structure of compound **6a**, showing thermal ellipsoids at 50% probability.

Crystals of compound **6c** were also obtained from $CHCl_3$/pentane by slow evaporation. Compound **6c** crystallized in the centrosymmetric monoclinic space group $P2_1/c$, with the asymmetric unit consisting of one azathia[7]helicene mole-

Figure 3. Asymmetric unit of the crystal structure of compound **6c**, showing thermal ellipsoids at 50% probability. The chloroform solvent molecule is omitted.

cule (Figure 3; for atom labeling, see Supporting Information). Whereas in the structure of compound **6a**, the ethoxyl groups are oriented differently, in the structure of compound **6c** they are coplanar with the thiophene ring. The distortion of the azathia[7]helicene molecule, defined by the sum of the three dihedral angles C6-C11-C14-C19, C11-C14-C19-C22, and C14-C19-C22-C27, is comparable (65.9°) to those of 5,10-diaza[5]helicene[16] and functionalized 6,9-dichloro- and 6,9-dimethoxy-5,10-diaza[5]helicenes.[12] Similar to the crystal packing of **6a**, the azathia[7]helicene molecules also form columnar stacks, along the [100] direction, featuring intermolecular π–π interactions inside the columns between two symmetry-equivalent benzene rings C13-C14/C16-C19, leading to an anti-parallel stacking between central aromatic rings (Figure 4). Additionally, intramolecular

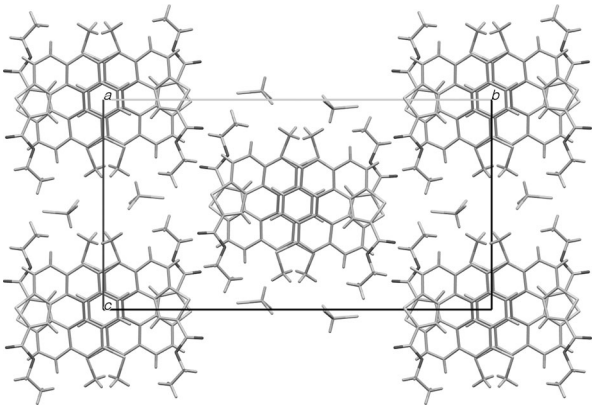

Figure 4. Packing in the crystal structure of compound **6c** along the [100] direction, showing the columnar, antiparallel stacking between central aromatic rings. H atoms are omitted for clarity.

π–π interactions are observed between the two thiophene rings S1/C4–C7 and S4/C26–C29 (3.485(2) Å between the ring centroids), as well as between thiophene ring S1/C4–C7 and benzene ring C21-C22/C24-C27 (3.987(2) Å between the ring centroids), which is not the case in the structure of **6a**. One $CHCl_3$ solvent molecule could be unambiguously observed, and is positioned between the column stacks.

Functionalization of diazadithia[7]helicenes: Dichloro diazadithia[7]helicene **6a** was synthesized in good yield, and the presence of chloro groups opened an opportunity for further functionalization. A variety of O-, S-, N-, and C-centered nucleophiles can be bound to the diazadithiahelicene platform. As a proof of concept for our previously reported methodology[12] we attempted to substitute the helicene core by nucleophilic aromatic substitution, palladium-catalyzed Suzuki coupling, and Buchwald–Hartwig amination (Scheme 4).

We first tested the S_NAr reaction of an O nucleophile. The S_NAr reaction of 4-*tert*-butylphenol (2.5 equiv) with 7,10-dichlorodiazadithia[7]helicene furnished product **7a** in 69% yield (Table 1, entry 1). Next, we explored the Suzuki and Buchwald–Hartwig amination reactions. Substitution of

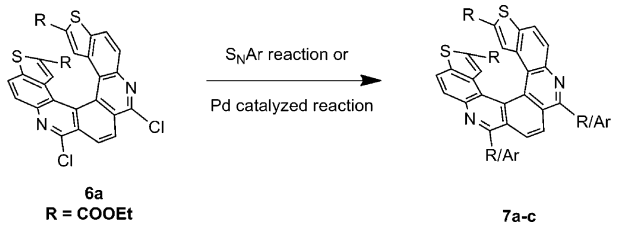

Scheme 4. S_NAr and palladium-catalyzed Suzuki coupling and Buchwald–Hartwig amination.

Table 1. Functionalization by S_NAr and palladium-catalyzed Suzuki coupling and Buchwald–Hartwig amination reactions.

Entry	Reagents and conditions	Diazadithia-[7]helicene	Yield [%]
1	**5a**, 4-*tert*-butylphenol, K_2CO_3, DMF, 80 °C, 12 h	**7a**	69
2	**5a**, *p*-tolylboronic acid, 5 mol% [Pd-$(PPh_3)_4$], aq. $NaHCO_3$, MeOH, toluene, reflux, 12 h	**7b**	58
3	**5a**, aniline, 5 mol% $Pd(OAc)_2$, Cs_2CO_3, *rac*-BINAP[a], toluene, 80 °C, 12 h	**7c**	65

[a] BINAP: 2,2′-bis(diphenylphosphino)-1,1′-binaphthyl.

both chloro groups at the 7- and 10-positions of the diazadithia[7]helicene was done by Suzuki cross-coupling. Aryl groups were introduced on the helicene skeleton by Pd-catalyzed reaction with *p*-tolylboronic acid, which yielded 58% of the desired product **7b** (Table 1, entry 2). Next, we attempted substitution with aniline under Buchwald–Hartwig amination conditions. Palladium-catalyzed reaction of 7,10-dichlorodiazadithia[7]helicene with aniline furnished the desired product **7c** in 65% yield (Table 1, entry 3).

Resolution by diastereomer separation: Buchwald–Hartwig amination of the racemic helicene skeleton with a chiral amine results in the formation of diastereomers, which then can easily be separated by column chromatography.[12] Thus, palladium-mediated amination of **6a** with L-(−)-α-methylbenzylamine, Cs_2CO_3, 5 mol% of $Pd(OAc)_2$ and *rac*-BINAP in toluene furnished the desired product **7d** in 74% yield as a 1:1 mixture of diastereomers (*M*,*S*,*S*/*P*,*S*,*S* = 1:1; the ratio of isomers was determined by integration of the NMR spectra; Scheme 5). The diastereomers were readily separated by chromatography on a silica-gel column and were configurationally very stable at room temperature. The diastereomers were completely characterized by NMR spectroscopy, HRMS and CD spectroscopy.

Racemization barrier: Racemization studies were performed on compound **6c**. Enantiopure forms were obtained by HPLC separation on a ChiralPak IA chiral column at room temperature and a flow rate of 0.7 mL min^{-1}. The mobile phase was heptane/ethanol (60:40 v/v) under isocratic conditions. Enantiomerically enriched [7]helicene **6c** racemizes in the solid state with a half-life of (6.5 ± 0.7) h at 220 °C. The corresponding free-energy barrier of racemization is

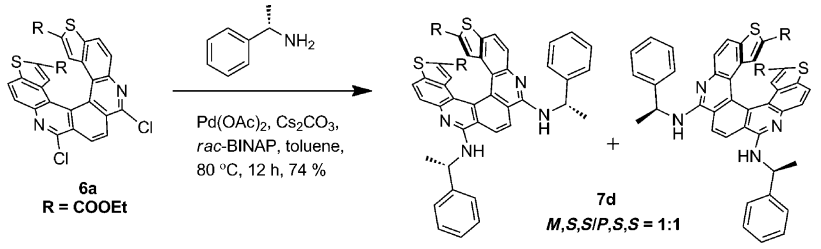

Scheme 5. Resolution through diastereomer separation.

(40.26 ± 0.14) kcal mol^{-1} (see Supporting Information). These values are similar to those reported for all-phenylene [7]helicene.[17]

UV/Vis absorption spectroscopy, fluorescence spectroscopy, circular dichroism spectroscopy, and cyclic voltammetry: The absorption and emission spectra of enantiomers **6c** and the absorption spectrum of diastereomers **7d** in chloroform are shown in Figure 5. The absorption spectrum of **6c** shows

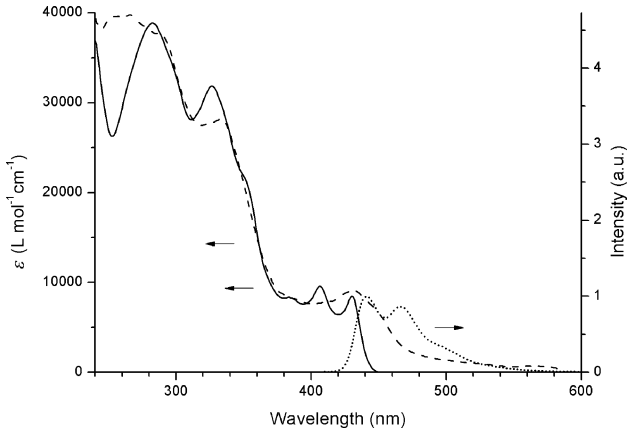

Figure 5. Absorption (solid) and emission (dotted) spectra of enantiomers **6c** and absorption (dashed) spectrum of diastereomers **7d** in chloroform.

three initial absorption peaks, located at 430, 407, and 383 nm and attributed tentatively to the vibronic progression of the $S_0 \rightarrow S_1$ transition, followed by a steep rise attributed to $S_0 \rightarrow S_n$ transitions. The molar extinction coefficient ε is 8500 L mol^{-1} cm^{-1} at 430 nm. The absorption spectrum of diastereomers **7d** is similar to that of enantiomers **6c**, except for a bathochromic shift and broadening of the initial peaks. Thus, it is difficult to clearly distinguish individual vibronic transitions, but we can still see a maximum at 432 nm ($\varepsilon = 9700$ L mol^{-1} cm^{-1}) and a shoulder at 451 nm.

The fluorescence spectrum of **6c** consists of a single transition with vibronic progression, of which the first two maxima are located at 441 and 465 nm. This corresponds to a vibrational spacing of (1170 ± 100) cm^{-1} in the ground state. The fluorescence quantum yield of **6c** in chloroform, determined by using perylene as reference ($\lambda_{ex} = 404$ nm), was $(2.3 \pm 0.2)\%$. This relatively low value suggests that non-radiative decay is rather efficient in these helicenes. The fluorescence decay time of **6c** in chloroform, determined by single-photon timing (see Supporting Information) was 0.36 ns. This leads to a fluorescence rate constant of $(6.4 \pm 0.6) \times 10^7$ s^{-1}, which is about ten times smaller than the value expected for a completely allowed transition ($f = 1$). On the other hand, for the non-radiative decay a rate constant of $(2.7 \pm 0.3) \times 10^9$ s^{-1} was obtained. This value is quite large for a relatively rigid molecule for which no low-lying nπ^* triplet states are expected.

Figure 6 shows the CD spectrum of enantiomers **6c** and diastereomers **7d** in chloroform. The CD spectrum of enantiomer (+)-**6c** starts with a small negative peak, followed by several large positive bands ($\lambda_{max} = 355$ nm) and a series of

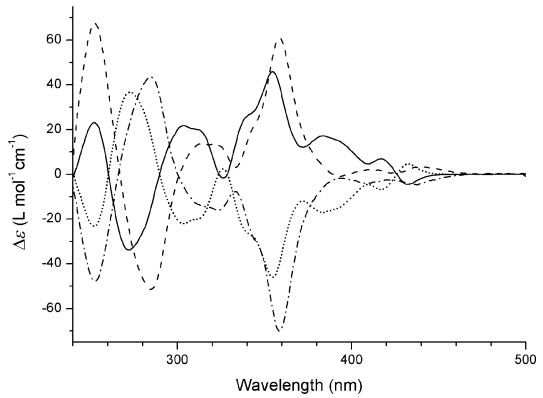

Figure 6. CD spectra of enantiomers *P*-(+)-**6c** (solid) and *M*-(−)-**6c** (dotted) and diastereomers *P*-(+)-**7d** (dashed) and *M*-(−)-**7d** (dashed-dotted).

alternating negative and positive bands below 340 nm. As expected, the spectrum for enantiomer (−)-**6c** is the mirror image of this. It is commonly accepted that the sign of the most intense CD band (β band) is representative of the absolute configuration of the helicene, with a positive (negative) band corresponding to *P* (*M*) helicity.[18b] Thus, we can attribute *P* helicity to enantiomer (+)-**6c**, and vice versa.

As the maxima at 430, 407 and 383 nm were attributed to a vibronic progression of the $S_0 \rightarrow S_1$ transition, one would expect them to all have the same sign in the CD spectrum; this is clearly not the case. For helicenes the red edge of the absorption spectrum is known to consist of two bands, namely, the p and α bands, which can have opposite signs in a CD spectrum.[18] This suggests that the maximum at 430 nm is due to the 0–0 transition of the α band (in this case the $S_0 \rightarrow S_1$ transition), while the maxima at 407 and 383 nm must be attributed to the 0–0 and 0–1 transition of the p band. This yields a vibronic progression of (1530 ± 100) cm^{-1} for the p band. However, since the CD intensity is much larger for the α band than for the p band,[18] it

cannot be excluded that the three observed vibrational maxima must be attributed to the p band and that the negative CD signal at long wavelengths reflects simply an α band hidden under the p band. Due to better conjugation, the absorption spectrum of **6c** is situated at much longer wavelength than those of the corresponding carbon–sulfur helicenes described by Rajca and co-workers, in which only cross-conjugation is possible. It is also slightly red-shifted compared to a [7]helicene in which thiophene rings alternate with benzene rings.[18b] The spectra of the diastereomers are largely similar, but display a bathochromic shift and have the same sign over the complete band of lowest-energy transitions, which leads to a disappearance of the initial small peak of opposite sign. Following the same arguments used for compound **6c**, we can attribute *P* helicity to diastereomer (+)-**7d**, and vice versa. The fact that the negative band at long wavelengths has disappeared suggests that for **7d** the 0–0 transition of the p band is now lower in energy than that of the α band. It is also noteworthy that, from roughly 300 nm onwards, diastereomers (+)-**7d** and (−)-**7d** display a difference in intensity on top a mere sign change. This is likely related to the (−)-α-methylbenzylamine side chains, which start to contribute to the spectrum.

Figure 7 shows the cyclic voltammogram for compound **6c** in acetonitrile/toluene (3:1) containing 0.1 M $TBAPF_6$ as supporting electrolyte. Within the available potential window of the chosen supporting electrolyte/solvent system, a single reversible reduction was observed at a potential of

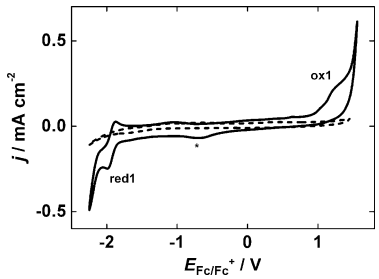

Figure 7. Cyclic voltammogram of **6c** in acetonitrile/toluene (3:1) at a nominal concentration of 0.8 mM (solid gray). Supporting electrolyte: 0.1 M $TBAPF_6$; scan rate: 200 mV s^{-1}. The black dashed trace shows the base electrolyte response.

$E_{1/2}(\text{red1}) = (-1.93 \pm 0.02)$ V. At positive potentials, a totally irreversible oxidation feature is found at approximately $E_{onset}(\text{ox1}) = (+1.03 \pm 0.03)$ V (see Supporting Information). A shallow peak at about −0.7 V, indicated by an asterisk, may be related to adsorption of a reaction product. From the redox potentials of **6c**, a HOMO–LUMO gap of (2.96 ± 0.05) eV can be estimated under the stated experimental conditions. This gap is only slightly larger than the optical band gap of 2.85 eV determined from the intersection of the normalized absorption and emission spectra, and therefore these values are more similar than is typically observed.[19a,b] Assuming in the simplest case that these energy levels are indeed responsible for the observed oxidation and reduction,[19c] using the electrochemically determined HOMO–LUMO gap and the empirical relationship $E_{HOMO} = (-1.4\,E_{onset}(\text{ox1}) - 4.6)$ eV,[19d] we can also estimate the HOMO and LUMO energies as −6.0 and −3.2 eV, respectively, relative to the vacuum level. The position of the HOMO will make hole injection from most common hole-injection electrodes (poly(3,4-ethylenedioxythiophene) or indium tin oxide) quite difficult. The position of the LUMO, on the other hand, is below the Fermi energy of Ca and other electropositive metal electrodes. Furthermore, the presence of an irreversible oxidation feature suggests that hole conduction may be accompanied by permanent chemical changes and premature failure of the device. Therefore, this compound may be better suited as an electron conductor when used for possible applications in organic electronics.

Conclusion

We have developed an efficient method for synthesis and functionalization of a helicene skeleton by S_NAr and palladium-catalyzed coupling reactions, and thus expanded the scope of the methodology to higher helicenes. The chiral forms obtained as a result of diastereomeric separation were conformationally very stable at room temperature and were characterized by NMR and CD spectroscopy. This methodology of functionalization and resolution has led to further exploration of the applications of azathiahelicenes. The role of diazadithia[7]helicenes as chiral inducers in asymmetric synthesis will also be investigated. We envisage potential applications of these helicenes in organic electronics.

Experimental Section

General experimental methods: NMR spectra were acquired on commercial instruments (Bruker Avance 300 MHz and Bruker AMX 400 MHz and 600 MHz) and chemical shifts (δ) are reported in parts per million (ppm) referenced to tetramethylsilane (^1H) or the internal (NMR) solvent signal (^{13}C). Mass spectra were run on a HP5989A apparatus (EI, 70 eV ionization energy) with Apollo 300 data system, a Micromass Quattro II apparatus (ESI) with MASSLYNX data system or a Thermo Finnigan LCQ Advantage apparatus (ESI/APCI). Exact mass measurements were carried out with a Kratos MS50TC instrument (performed in EI mode at a resolution of 10000). Melting points (not corrected) were determined by using a Reichert Thermovar apparatus. UV/Vis absorption spectra and emission spectra were respectively taken on a PerkinElmer Lambda 40 spectrophotometer and a Horiba Jobin Yvon Fluorolog-3-22 spectrofluorometer. The fluorescence spectra are corrected for the wavelength dependence of the sensitivity of the detection part. CD measurements were performed on a Jasco J600 spectropolarimeter. All spectroscopic measurements were performed in quartz cuvettes with an optical path length of 1 cm. For column chromatography, 70–230 mesh silica 60 (E. M. Merck) was used as the stationary phase. Chemicals received from commercial sources were used without further purification. K_2CO_3 (anhydrous, granulated) was finely ground (with mortar and pestle) prior to use. All solvents were used as received from commercial sources and not explicitly dried prior to use (≤0.1% H_2O). All photochemical reactions were performed in the Rayonet photochemical reactor equipped with interchangeable light sources (250, 300, and 350 nm lamps).

Single-photon timing (SPT): Fluorescence decay times were determined by SPT measurements and the setup has been described in detail previously.[20] A time-correlated single-photon counting PC module (SPC 830, Becker & Hickl) was used to obtain the fluorescence decay histogram in 4096 channels. The decays were recorded with 10000 counts in the peak channel in time windows of 6.6 ns corresponding to 1.6 ps per channel and analyzed with time-resolved fluorescence analysis software (FAST) based on iterative reconvolution with a Goldin algorithm. The full width at half-maximum (FWHM) of the instrument response function was typically on the order of 40 ps. The quality of the fits was judged by the random distribution of the residuals and by the value of the reduced chi-squared parameter ($\chi^2 < 1.1$).[21] All measurements were performed in quartz cuvettes with an optical path length of 1 cm at an optical density of ca. 0.1 at the excitation wavelength of 430 nm.

Cyclic voltammetry: Acetonitrile ($\geq$ 99.8%, H_2O <0.001%, Sigma-Aldrich) and toluene (HPLC grade, Sigma-Aldrich) were used as received, whereas tetra-*n*-butylammonium hexafluorophosphate ($TBAPF_6$, electrochemical grade, Fluka) was dried overnight in vacuo at 110°C. For solubility reasons, the electroactive substance (*rac*-diazadithia[7]helicene **6c**) was dissolved in acetonitrile/toluene (3:1). Electrochemical measurements were carried out in a custom-made single-compartment three-electrode cell with a working volume of 1 cm^3, containing a Pt coil counter-electrode. The reference electrode was a laboratory-built non-aqueous $Ag|Ag^+$ electrode, contacted to the cell through a porous glass diaphragm, and was calibrated versus ferrocene after the measurements. All potentials are given with reference to the ferrocene equilibrium potential. The working electrode (WE) was a polycrystalline Pt bead, polished to mirror finish, exposing a geometric surface area of 0.032 cm^2 in hanging-meniscus configuration. The WE was annealed with a butane flame before every measurement and cooled in a stream of high-purity Ar. The potentiostat was a software-controlled Autolab PGSTAT101 system (Metrohm Autolab BV, The Netherlands). In all cases, the WE was brought into contact with the electrolyte under potential control at a potential within the stability range of the studied compound. Before and during the measurements, solutions were kept under a solvent-saturated Ar (purity 5.0, Praxair) atmosphere.

Synthesis of ethyl 7-chloro-8-formylthieno[3,2-*f*]quinoline-2-carboxylate (1): $POCl_3$ (13.9 mL, 151.9 mmol) was added dropwise over a period of 15 min to dimethylformamide (DMF) (3.8 mL, 53.17 mmol) at 0°C. The resulting Vilsmeier salt was stirred for 10 min at 0°C, and then ethyl 5-acetamidobenzo[*b*]thiophene-2-carboxylate (4.0 g, 15.19 mmol) was added and reaction mixture heated to 80°C. After 15 h, reaction mixture was quenched with ice water and extracted with CH_2Cl_2. The organic layer was separated, washed with brine, dried over anhydrous $MgSO_4$, and evaporated to dryness to furnish compound **1** (4.25 g, 87%) as yellow powder. M.p. 209–211°C; MS (EI): *m*/*z* 320 $[M+H]^+$; HRMS (EI) calcd for $C_{15}H_{10}NO_3ClS$: 319.0070; found: *m*/*z* 319.0098; ^1H NMR (300 MHz, $CDCl_3$): $\delta = 10.62$ (s, 1H, CHO), 9.18 (s, 1H, ArH), 8.69 (s, 1H, ArH), 8.24 (d, 1H, $J = 9.0$ Hz, ArH), 8.05 (d, 1H, $J = 9.06$ Hz, ArH), 4.47 (q, 2H, $J = 7.1$ Hz, OCH_2), 1.47 ppm (t, 3H, $J = 7.1$ Hz, CH_3); ^{13}C NMR (75 MHz, $CDCl_3$, 25°C, TMS): $\delta = 189.1$ (CHO), 162.1, 150.2, 149.1, 141.7, 137.1, 135.8, 135.1, 128.4, 127.5, 127.4, 126.4, 123.6 (C, CH), 62.2, 14.4 ppm (CH_2, CH_3).

Synthesis of ethyl 8-formyl-7-(methylthio)thieno[3,2-*f*]quinoline-2-carboxylate (2): NaSMe (0.438 g, 6.25 mmol) was added to a solution of compound **1** (1.0 g, 3.12 mmol) in DMF, and the reaction mixture stirred at room temperature for 2 h, quenched with water, and extracted with CH_2Cl_2. The organic layer was separated, washed with brine, dried over anhydrous $MgSO_4$, and evaporated to dryness to furnish compound **2** (0.805 g, 78%) as a yellow powder. M.p. 202–204°C; MS (EI): *m*/*z*: 332 $[M+H]$; HRMS (EI) calcd for $C_{16}H_{13}NO_3S_2$ 331.0337; found: *m*/*z* 331.0338; ^1H NMR (300 MHz, $CDCl_3$): $\delta = 10.43$ (s, 1H, CHO), 8.90 (s, 1H, ArH), 8.63 (s, 1H, ArH), 8.14 (d, 1H, $J = 9.0$ Hz, ArH), 7.99 (d, 1H, $J = 9.0$ Hz, ArH), 4.46 (q, 2H, $J = 7.1$ Hz, OCH_2), 2.75 (s, 3H, SCH_3), 1.46 ppm (t, 3H, $J = 7.1$ Hz, CH_3); ^{13}C NMR (75 MHz, $CDCl_3$, 25°C, TMS): $\delta = 189.8$ (CHO), 162.4, 159.9, 149.0, 140.3, 136.7, 136.3, 135.8, 127.9, 127.5, 127.4, 127.1, 121.1 (C, CH), 62.1, 14.4, 13.2 ppm (CH_2, CH_3).

Synthesis of ethyl 7-chloro-8-(hydroxymethyl)thieno[3,2-*f*]quinoline-2-carboxylate (3a): general procedure: Sodium borohydride (0.065 g, 1.72 mmol) was added to a stirred solution of aldehyde **1** (0.500 g, 1.56 mmol) in THF (50 mL) and MeOH (10 mL), and the reaction mixture stirred at 0°C for 30 min. The reaction mixture was quenched with water and diluted with Et_2O, and the organic layer was separated, washed with brine, dried over anhydrous $MgSO_4$, and evaporated to dryness to give **3a** (0.425 g, 85%) as a white solid. The product was used without further purification. M.p. 225–227°C; MS (EI): *m*/*z*: 322 $[M+H]$; HRMS (EI) calcd for $C_{15}H_{12}ClNO_3S$: 321.0226; found: *m*/*z* 321.0039; ^1H NMR (300 MHz, $[D_6]DMSO$): $\delta = 9.06$ (s, 1H, ArH), 8.90 (s, 1H, ArH), 8.36 (d, 1H, $J = 9.2$ Hz, ArH), 7.97 (d, 1H, $J = 9.0$ Hz, ArH), 5.70 (t, 1H, $J = 5.6$ Hz, OH), 4.75 (d, 2H, $J = 5.2$ Hz, CH_2OH), 4.42 (q, 2H, $J = 7.1$ Hz, OCH_2), 1.38 ppm (t, 3H, $J = 7.1$ Hz, CH_3); ^{13}C NMR (75 MHz, $CDCl_3$, 25°C, TMS): $\delta = 161.7$, 148.1, 144.8, 140.5, 134.8, 134.5, 132.7, 128.6, 127.2, 125.2, 123.8 (C, CH), 61.6, 60.2, 14.1 ppm (CH_2, CH_3).

Synthesis of ethyl 8-(hydroxymethyl)-7-(methylthio)thieno[3,2-*f*]quinoline-2-carboxylate (4a): Synthesis according to general procedure leading to **3a** (see the Supporting Information).

Synthesis of ethyl 8-(bromomethyl)-7-chlorothieno[3,2-*f*]quinoline-2-carboxylate (3b): general procedure: Phosphorus tribromide (0.149 mL, 1.58 mmol) was added to a solution of compound **3a** (0.425 g, 1.32 mmol) in THF (50 mL) and the reaction mixture cooled to 0°C. The reaction mixture was stirred at room temperature for 5 h and then quenched with water. The organic layer was separated, washed with brine, dried over anhydrous $MgSO_4$, evaporated to dryness, and purified by column chromatography with EtOAc/petroleum ether (20:80) as eluent to furnish compound **3b** (0.301 g, 59%) as a white solid. M.p. 192–193°C; MS (EI): *m*/*z*: 383 $[M+H]$; HRMS (EI) calcd for $C_{15}H_{11}ClBrNO_2S$: 382.9382; found: *m*/*z* 382.9364; ^1H NMR (300 MHz, $[D_6]DMSO$): $\delta = 9.49$ (s, 1H, ArH), 8.95 (s, 1H, ArH), 8.45 (d, 1H, $J = 9.0$ Hz, ArH), 8.01 (d, 1H, $J = 9.0$ Hz, ArH), 4.90 (s, 2H, CH_2Br), 4.41 (q, 2H, $J = 7.1$ Hz, OCH_2), 1.38 ppm (t, 3H, $J = 7.1$ Hz, CH_3); ^{13}C NMR (75 MHz, $CDCl_3$, 25°C, TMS): $\delta = 161.6$, 140.9, 136.2, 135.1, 134.7, 132.6, 128.7, 127.1, 126.6, 123.7 (C, CH), 61.7, 14.1 ppm (CH_2, CH_3).

Synthesis of ethyl 8-(bromomethyl)-7-(methylthio)thieno[3,2-*f*]quinoline-2-carboxylate (4b): Synthesis according to procedure leading to **3b** (see Supporting Information).

Synthesis of ethyl 8-[(bromotriphenylphosphoranyl)methyl]-7-chlorothieno[3,2-*f*]quinoline-2-carboxylate 3c: general procedure: Triphenylphosphine (0.616 g, 2.35 mmol) was added to a solution of compound **3b** (0.301 g, 0.78 mmol) in toluene, the reaction mixture heated to reflux for 12 h and cooled to room temperature, and the resulting solid isolated by filtration, washed with pentane, and dried under vacuum to furnish phosphonium salt **3c** (0.434 g, 86%) as a white solid. M.p. 239–241°C; MS (EI): *m*/*z*: 646 $[M+H]$ (observed $[M-Br]=566$); HRMS (EI) calcd for $C_{33}H_{26}ClBrNO_2SP$ 645.0294; found: *m*/*z* 566.1106 $[M-Br]$; ^1H NMR (300 MHz, $CDCl_3$): $\delta = 8.29$ (d, 1H, $J = 8.4$ Hz, ArH), 8.05 (d, 1H, $J = 9.2$ Hz, ArH), 7.89–7.79 (m, 10H, ArH), 7.71–7.64 (m, 7H, ArH), 6.10–6.05 (m, 2H, CH_2P), 4.46 (q, 2H, $J = 7.1$ Hz, OCH_2), 1.48 ppm (t, 3H, $J = 7.1$ Hz, CH_3); ^{13}C NMR (75 MHz, $CDCl_3$, 25°C, TMS): $\delta = 162.2$, 135.6, 134.7, 134.6, 134.5, 130.6, 130.5, 117.8, 116.7 (C, CH), 62.0, 14.5 ppm (CH_2, CH3).

Synthesis of ethyl 8-[(bromotriphenylphosphoranyl)methyl]-7-(methylthio)thieno[3,2-*f*]quinoline-2-carboxylate (4c): See Supporting Information.

Synthesis of diethyl 8,8′-(ethene-1,2-diyl)bis(7-chlorothieno[3,2-*f*]quinoline-2-carboxylate) 5a: general procedure: A solution of 7-chloro-8-formylthieno[3,2-*f*]quinoline-2-carboxylate (**1**; 0.155 g, 0.49 mmol) was added dropwise to a stirred solution of phosphonium salt **3c** (0.350 g, 0.54 mmol) and potassium *tert*-butoxide (0.082 g, 0.73 mmol) in THF at 0°C, after which the reaction mixture was stirred for 6 h. The solvent was removed under reduced pressure and a mixture of CH_2Cl_2 and MeOH was added to give a precipitate, which was collected by filtration and dried in vacuo to give **5a** (0.170 g, 58%) as a yellow solid. Compound **5a** was difficult to characterize by NMR spectroscopy due to its poor solubility. M.p. 189–190°C; MS (EI): *m*/*z*: 607 $[M+H]$; HRMS (EI) calcd for $C_{30}H_{20}Cl_2N_2O_4S_2$: 606.0242; found: *m*/*z* 607.0302 $[M+H]$.

Synthesis of ethyl 7-chloro-8-{2-[2-(ethoxycarbonyl)-7-(methylthio)-thieno[3,2-*f*]quinolin-8-yl]vinyl}thieno[3,2-*f*]quinoline-2-carboxylate 5b: Synthesis according to procedure leading to **5a** (see Supporting Information)

Synthesis of diethyl 8,8′-(ethene-1,2-diyl)bis[7-(methylthio)thieno[3,2-*f*]quinoline-2-carboxylate] 5c: Synthesis according to procedure leading to **5a** (see Supporting Information)

Synthesis of 7,10-dichloro-6,11-diaza-3,14-dithia[7]helicene-2,15-bis(carboxylate) (6a): general procedure: Iodine (0.073 g, 0.28 mmol) was added to a solution of compound **5a** (0.169 g, 0.26 mmol, mixture of two isomers) in toluene (265 mL). Argon was bubbled through the solution for 30 min, and then an excess of propylene oxide was added to the solution. The reaction mixture was irradiated in a Rayonet photochemical reactor ($\lambda = 350$ nm) for 15 h, after which it was washed with aqueous $Na_2S_2O_3$, water, and brine, dried over anhydrous $MgSO_4$, and evaporated to afford a dark yellow residue. Purification by column chromatography with EtOAc/petroleum ether (20:80) as eluent gave the racemic helicene **6a** (0.090 g, 56%) as a light yellow solid. M.p. 230–232°C; MS (EI): *m/z*: 605 [*M*+H]; HRMS (EI) calcd for $C_{30}H_{18}Cl_2N_2O_4S_2$: 604.0085; found: *m/z* 605.0305; ^{1}H NMR (300 MHz, $CDCl_3$): $\delta = 8.85$ (s, 2H, ArH), 8.26 (d, 2H, $J = 8.6$ Hz, ArH), 8.08 (d, 2H, $J = 8.8$ Hz, ArH), 6.87 (s, 2H, ArH), 4.26 (m, 2H, OCH_2), 4.12 (m, 2H, OCH_2), 1.30 ppm (m, 6H, CH_3); ^{13}C NMR (75 MHz, $CDCl_3$, 25°C, TMS): $\delta = 161.6$, 150.2, 143.9, 143.8, 142.7, 133.7, 133.1, 129.3, 129.2, 128.9, 128.0, 127.3, 126.8, 125.1, 121.1 (C, CH), 61.6, 14.4 ppm (CH_2, CH_3).

Synthesis of 7-chloro, 10-thiomethoxy-6,11-diaza-3,14-dithia[7]helicene-2,15-bis(carboxylate) 6b: Synthesis according to procedure leading to **6a** (see Supporting Information)

Synthesis of 7,10-bis(thiomethoxy)-6,11-diaza-3,14-dithia[7]helicene-2,15-bis(carboxylate) 6c: Synthesis according to procedure leading to **6a** (see Supporting Information).

Nucleophilic substitution reaction: synthesis of 7,10-bis(*tert*-butylphenyl)-6,11-diaza-3,14-dithia[7]helicene-2,15-bis(carboxylate) (7a): K_2CO_3 (11.3 mg, 0.082 mmol) and *tert*-butylphenol (12.3 mg, 0.082 mmol) were added to a solution of **6a** (20 mg, 0.03 mmol) in DMF (10 mL), and the reaction mixture was stirred at 80°C for 12 h. Subsequently, the mixture was diluted with ethyl acetate (20 mL) and washed with distilled water (3×20 mL). The organic fraction was dried over $MgSO_4$ and filtered, and the solvent was removed under vacuum. After column chromatographic purification with EtOAc/petroleum ether (15:75) as eluent, substituted helicene **7a** (19 mg, 69%) was obtained as a yellow solid. M.p. 327–329°C; MS (EI): *m/z*: 833 [*M*+H]; HRMS (EI) calcd for $C_{50}H_{44}N_2O_6S_2$: 832.4621; found: *m/z* 833.2715 [M+H]; ^{1}H NMR (300 MHz, $CDCl_3$): $\delta =$ 8.91 (s, 2H, ArH), 8.00 (d, 2H, $J = 8.8$ Hz, ArH), 7.92 (d, 2H, $J = 8.6$ Hz, ArH), 7.55 (d, 4H, $J = 8.2$ Hz, ArH), 7.43 (d, 4H, $J = 8.4$ Hz, ArH), 7.00 (s, 2H, ArH), 4.24–4.08 (m, 4H, OCH_2), 1.43 (s, 18H, *t*Bu), 1.28–1.26 ppm (m, 6H, CH_3); ^{13}C NMR (75 MHz, $CDCl_3$, 25°C, TMS): $\delta =$ 162.1, 158.4, 151.4, 148.0, 142.2, 140.5, 133.6, 132.2, 130.1, 129.8, 128.1, 126.5, 124.0, 123.8, 122.6, 121.2, 120.0 (C, CH), 61.3, 34.7, 31.7, 14.5 ppm (CH_2, CH_3).

Palladium-catalyzed Suzuki coupling: synthesis of 7, 10-bis(4-methylphenyl)-6,11-diaza-3,14-dithia[7]helicene-2,15-bis(carboxylate) (7b): [Pd(PPh_3)$_4$] (3 mg, 5 mol%) was added to a solution of **6a** (20 mg, 0.03 mmol) in toluene (20 mL), and to the resulting solution *p*-tolylboronic acid (13 mg, 0.099 mmol) in aqueous $NaHCO_3$ (10 mg, 0.228 mmol) and MeOH (0.5 mL) were added. The reaction mixture was heated to reflux for 12 h. Subsequently, the mixture was washed with distilled water (3×20 mL). The organic fraction was dried over $MgSO_4$ and filtered, and the solvent was removed under vacuum. After column chromatographic purification with EtOAc/petroleum ether (20:80) as eluent, substituted helicene **7b** (14 mg, 58%) was obtained as a yellow solid. M.p. 255–257°C; MS (EI): *m/z*: 717 [*M*+H]; HRMS (EI) calcd for $C_{44}H_{32}N_2O_4S_2$: 716.1803; found: *m/z* 717.1865 [*M*+H]; ^{1}H NMR (300 MHz, $CDCl_3$): $\delta =$ 8.41 (d, 2H, $J = 8.6$ Hz, ArH), 8.35 (s, 2H, ArH), 8.07 (d, 2H, $J = 8.6$ Hz, ArH), 7.79 (d, 2H, $J = 7.7$ Hz, ArH), 7.44 (d, 2H, $J = 7.7$, ArH), 7.07 (s, 2H, ArH), 4.29–4.23 (m, 2H, OCH_2), 4.21- 4.08 (m, 2H, OCH_2), 2.52 (s, 6H, ArH-CH_3), 1.31–1.25 ppm (m, 6H, CH_3); ^{13}C NMR (75 MHz, $CDCl_3$, 25°C, TMS): $\delta = 162.1$, 159.5, 143.7, 142.2, 139.3, 136.4, 133.3, 132.7, 130.5, 129.6, 129.5, 129.4, 128.2, 126.8, 126.7, 124.1, 121.3 (C, CH), 61.4, 21.5, 14.4 ppm (CH_2, CH_3).

Buchwald–Hartwig amination: synthesis of 7,10-bis(phenylamino)-6,11-diaza-3,14-dithia[7]helicene-2,15-bis(carboxylate) (7c): Aniline (7.6 mg, 0.08 mmol), Cs_2CO_3 (98 mg, 0.3 mmol), *rac*-BINAP (1.0 mg, 0.0015 mmol), and $Pd(OAc)_2$ (0.3 mg, 0.0015 mmol) were added to a solution of **6a** (20 mg, 0.03 mmol) in toluene (10 mL), and the reaction mixture was stirred at 80°C for 12 h. Subsequently, the mixture was diluted with ethyl acetate (20 mL) and washed with distilled water (3×20 mL). The organic fraction was dried over $MgSO_4$ and filtered and the solvent was removed under vacuum. After column chromatographic purification with EtOAc/petroleum ether (40:60) as eluent, substituted helicene **7c** (15.5 mg, 65%) was obtained as an orange solid. M.p. 325–327°C; MS (EI): *m/z*: 719 [*M*+H]; HRMS (EI) calcd for $C_{42}H_{30}N_4O_4S_2$: 718.1708; found: *m/z* 719.1774 [*M*+H]; ^{1}H NMR (300 MHz, [D$_6$]DMSO): $\delta = 9.75$ (s, 2H, NH), 9.04 (s, 2H, ArH), 8.14–8.09 (m, 6H, ArH), 7.92 (d, 2H, $J =$ 8.6 Hz, ArH), 7.49–7.44 (m, 4H, ArH), 7.15–7.10 (m, 2H, ArH), 6.91 (s, 2H, ArH), 4.21–4.02 (m, 4H, OCH_2), 1.24–1.20 ppm (m, 6H, CH_3); ^{13}C NMR (75 MHz, [D$_6$]DMSO, 25°C, TMS): $\delta = 161.4$, 150.8, 143.2, 141.0, 138.0, 132.9, 131.1, 128.8, 128.5, 127.6, 124.1, 122.5, 122.4, 121.9, 120.9, 117.6 (C, CH), 61.0, 14.1 ppm (CH_2, CH_3).

Synthesis of 7,10-bis[(*S*)-α-(methylbenzylamino)]-6,11-diaza-3,14-dithia[7]helicene-2,15-bis(carboxylate) (7d): (*S*)-α-Methylbenzylamine (30 μL, 0.268 mmol), Cs_2CO_3 (348 mg, 1.07 mmol), *rac*-BINAP (3.3 mg, 0.0053 mmol, 5 mol%) and $Pd(OAc)_2$ (1.2 mg, 0.0053 mmol, 5 mol%) were added to a solution of **6a** (65 mg, 0.107 mmol) in toluene (20 mL), and the reaction mixture was stirred at 80°C for 12 h. Subsequently, the mixture was diluted with ethyl acetate (20 mL) and washed with distilled water (3×20 mL). The organic fraction was dried over $MgSO_4$ and filtered, and the solvent was removed under vacuum. After column chromatographic purification with EtOAc/petroleum ether (20:80) as eluent, helicene **7d** (54 mg, 74%, 1:1 mixture of diastereomers) was obtained as a light yellow solid. M.p. 139–141°C; MS (EI): *m/z*: 775 [*M*+H]; HRMS (EI) calcd for $C_{46}H_{38}N_4O_4S_2$: 774.2334; found: *m/z* 775.2413 [M+H]; ^{1}H NMR (300 MHz, $CDCl_3$, diastereomer 2): $\delta = 8.05$ (s, 2H, ArH), 7.89 (d, 2H, $J = 8.8$ Hz, ArH), 7.76 (d, 2H, $J = 8.8$ Hz, ArH), 7.61–7.58(m, 4H, ArH), 7.40–7.35 (m, 4H, ArH), 7.30–7.27 (m, 2H, ArH), 7.01 (s, 2H, ArH), 5.87–5.82 (m, 2H, CH), 5.71–5.69 (m, 2H, NH), 4.27–4.08 (m, 4H, OCH_2), 1.85 (d, 6H, $J = 6.7$ Hz, $CHCH_3$), 1.34–1.25 ppm (m, 6H, CH_2CH_3).^{13}C NMR (75 MHz, $CDCl_3$, 25°C, TMS): $\delta = 162.5$, 151.8, 144.9, 144.5, 138.4, 133.6, 131.5, 129.8, 129.7, 127.3, 126.7, 123.7, 121.0, 119.9, 117.8 (C, CH), 61.1, 50.9, 22.3, 14.3 ppm (CH_2, CH_3).

Crystallographic data: For the structures of compounds **6a** and **6c**, X-ray intensity data were collected on a SMART 6000 diffractometer equipped with CCD detector by using $Cu_{K\alpha}$ radiation ($\lambda = 1.54178$ Å) and φ and ω scans. The images were interpreted and integrated with the program SAINT from Bruker.[22] Both structures were solved by direct methods and refined by full-matrix least-squares techniques on F^2 by using the SHELXTL program package.[23] Non-hydrogen atoms were anisotropically refined and the hydrogen atoms in the riding mode and isotropic temperature factors fixed at 1.2 U_{eq} of the parent atoms (1.5 U_{eq} for methyl groups). CCDC-925861 (**6a**) and CCDC-925862 (**6c**) contain the supplementary crystallographic data for this paper. These data can be obtained free of charge from The Cambridge Crystallographic Data Centre via www.ccdc.cam.ac.uk/data_request/cif.

Crystal data for compound 6a: $C_{30}H_{18}Cl_2N_2O_4S_2$, $M = 605.50$; orthorhombic, $Pca2_1$ (No. 29); $a = 22.657(10)$, $b = 12.435(5)$, $c = 18.362(3)$ Å; $V =$ 5173(3) Å^3; $T = 100(2)$ K; $Z = 8$; $\rho_{calcd} = 1.555$ g cm^{-3}; $\mu(Cu_{K\alpha}) =$ 4.128 mm^{-1}; $F(000) = 2480$; crystal size 0.5×0.2×0.1 mm; 8772 independent reflections ($R_{int} = 0.1014$). Final $R = 0.0968$ for 6981 reflections with $I > 2\sigma(I)$ and $wR2 = 0.2138$ for all data. Detection of a pseudo-center of symmetry suggested the centrosymmetric space group *Pbca*.[24] However, refinement of the structure in the latter space group converged to an *R* value of 17%, which is about twice that in space group $Pca2_1$. Therefore, $Pca2_1$ was kept as the preferred space group.

Crystal data for compound 6c: $C_{33}H_{25}Cl_3N_2O_4S_4$, $M = 748.18$; monoclinic, $P2_1/c$ (No. 14); $a = 7.5328(6)$, $b = 28.1374(16)$, $c = 15.6203(10)$ Å; $\beta =$ 103.576(3)°; $V = 3218.3(4)$ Å^3; $T = 100(2)$ K; $Z = 4$; $\rho_{calcd} = 1.544$ g cm^{-3}; μ-

($Cu_{K\alpha}$) = 5.363 mm^{-1}; $F(000)$ = 1536; crystal size 0.4 × 0.2 × 0.2 mm; 5591 independent reflections (R_{int} = 0.1604); final R = 0.0642 for 4193 reflections with $I > 2\sigma(I)$ and $wR2$ = 0.1720 for all data. The presence of a $CHCl_3$ solvent molecule was observed in the structure.

Acknowledgements

We thank the FWO (Fund for Scientific Research - Flanders), the K.U. Leuven through GOA 2011/2, and BELSPO through IAP-VI-27 and VII-05 for continuing financial support, the Hercules Foundation of the Flemish Government (Grant No. 20100225-7) for mass spectrometry. K. M. de Gooijer, K.V. Joosten-Gibcus, E. van Echten, M. W. van der Meijden, and Prof. R. M. Kellogg of Syncom B.V. are kindly acknowledged for the enantiomeric separation of helicenes by chiral HPLC. S.F.L.M. gratefully acknowledges the receipt of a Marie Curie European reintegration grant. A.C. is indebted to the IWT for financial support.

[1] a) A. Rajca, M. Miyasaka, *Synthesis and Characterization of Novel Chiral Conjugated Materials. Functional Organic Materials: Syntheses and Strategies*, (Eds.: T. J. J. Mueller, U. H. F. Bunz), Wiley-VCH, Germany, **2007**; pp. 543–577; b) Y. Shen, C.-F. Chen, *Chem. Rev.* **2012**, *112*, 1463–1535; c) I. G. Stara, I. Starý, *Sci. Synth.* **2010**, *45b*, 885–953; d) A. Rajca, S. Rajca, M. Pink, M. Miyasaka, *Synlett* **2007**, *14*, 2007; e) S. K. Collins, M. P. Vachon, *Org. Biomol. Chem.* **2006**, *4*, 2518–2524; f) A. Urbano, *Angew. Chem.* **2003**, *115*, 4116–4119; *Angew. Chem. Int. Ed.* **2003**, *42*, 3986–3989; g) F. Dumitrascu, D. G. Dumitrescu, I. Aron, *ARKIVOC (Gainesville, FL, U.S.)* **2010**, 1–32.

[2] a) T. J. Wigglesworth, D. Sud, T. B. Norsten, V. S. Lekhi, N. R. Branda, *J. Am. Chem. Soc.* **2005**, *127*, 7272–7273; b) E. Botek, B. Champagne, M. Turki, J.-M. Andre, *J. Chem. Phys.* **2004**, *120*, 2042–2048; c) C. Nuckolls, T. J. Katz, T. Verbiest, S. Van Elshocht, H.-G. Kuball, S. Kiesewalter, A. J. Lovinger, A. Persoons, *J. Am. Chem. Soc.* **1998**, *120*, 8656–8660.

[3] a) J. Rybacek, G. Huerta-Angeles, A. Kollarovic, I. G. Stara, I. Stary, P. Rahe, M. Nimmrich, A. Kuhnle, *Eur. J. Org. Chem.* **2011**, 853–860; b) C. Kim, T. J. Marks, A. Facchetti, M. Schiavo, A. Bossi, S. Maiorana, E. Licandro, F. Todescato, S. Toffanin, M. Muccini, C. Graiff, A. Tiripicchio, *Org. Electron.* **2009**, *10*, 1511–1520; c) W. Ichinose, M. Miyagawa, J. Z. An, M. Yamaguchi, *Org. Lett.* **2012**, *14*, 3123–3125; d) Z. An, M. Yamaguchi, *Chem. Commun.* **2012**, *48*, 7383–7385; e) K.-I. Shinohara, Y. Sannohe, S. Kaieda, K.-I. Tanaka, H. Osuga, H. Tahara, Y. Xu, T. Kawase, T. Bando, H. Sugiyama, *J. Am. Chem. Soc.* **2010**, *132*, 3778–3782; f) Y. Xu, Y. Zhang, H. Sugiyama, T. Umano, H. Osuga, K. Tanaka, *J. Am. Chem. Soc.* **2004**, *126*, 6566–6567.

[4] a) M. Gingras, *Chem. Soc. Rev.* **2013**, *42*, 968–1006; b) A. Urbano, M. C. Carreno, *Org. Biomol. Chem.* **2013**, *11*, 699–708.

[5] a) T. Caronna, S. Gabbiadini, A. Mele, F. Recupero, *Helv. Chim. Acta* **2002**, *85*, 1–8; b) C. Bazzini, S. Brovelli, T. Caronna, C. Gambarotti, M. Giannone, P. Macchi, F. Meinardi, A. Mele, W. Panzeri, F. Recupero, A. Sironi, R. Tubino, *Eur. J. Org. Chem.* **2005**, 1247–1257; c) M. Monteforte, S. Cauteruccio, S. Maiorana, T. Benincori, A. Forni, L. Raimondi, C. Graiff, A. Tiripicchio, G. R. Stephenson, E. Licandro, *Eur. J. Org. Chem.* **2011**, 5649–5658; d) D. Waghray, W. Nulens, W. Dehaen, *Org. Lett.* **2011**, *13*, 5516–5519; e) M. Weimar, R. Correa da Costa, F.-H. Lee, M. J. Fuchter, *Org. Lett.* **2013**, *15*, 1706–1709; f) K. Nakano, H. Oyama, Y. Nishimura, S. Nakasako, K. Nozaki, *Angew. Chem.* **2012**, *124*, 719–723; *Angew. Chem. Int. Ed.* **2012**, *51*, 695–699.

[6] K. E. S. Phillips, T. J. Katz, S. Jockusch, A. J. Lovinger, N. J. Turro, *J. Am. Chem. Soc.* **2001**, *123*, 11899–11907.

[7] a) M. R. Crittall, H. S. Rzepa, D. R. Carbery, *Org. Lett.* **2011**, *13*, 1250–1253; b) N. Takenaka, R. S. Sarangthem, B. Captain, *Angew. Chem.* **2008**, *120*, 9854–9856; *Angew. Chem. Int. Ed.* **2008**, *47*, 9708–9710; c) E. Murguly, R. McDonald, N. R. Branda, *Org. Lett.* **2000**, *2*, 3169–3172; d) S. Graule, M. Rudolph, N. Vanthuyne, J. Autschbach, C. Roussel, J. Crassous, R. Reau, *J. Am. Chem. Soc.* **2009**, *131*, 3183–3185.

[8] a) M. T. Reetz, E. W. Beuttenmuller, R. Goddard, *Tetrahedron Lett.* **1997**, *38*, 3211–3214; b) M. T. Reetz, S. Sostmann, *J. Organomet. Chem.* **2000**, *603*, 105–109; c) J. M. Fox, T. J. Katz, *J. Org. Chem.* **1999**, *64*, 302–305; d) A. Sudhakar, T. J. Katz, B. W. Yang, *J. Am. Chem. Soc.* **1986**, *108*, 2790–2791; e) T. J. Katz, A. Sudhakar, M. F. Teasley, A. M. Gilbert, W. E. Geiger, M. P. Robben, M. Wuensch, M. D. Ward, *J. Am. Chem. Soc.* **1993**, *115*, 3182–3198.

[9] D. C. Harrowven, I. L. Guy, L. Nanson, *Angew. Chem.* **2006**, *118*, 2300–2303; *Angew. Chem. Int. Ed.* **2006**, *45*, 2242–2245.

[10] a) J. Misek, F. Teply, I. G. Stara, M. Tichy, D. Saman, I. Cisarova, P. Vojtisek, I. Stary, *Angew. Chem.* **2008**, *120*, 3232–3235; *Angew. Chem. Int. Ed.* **2008**, *47*, 3188–3191; b) A. Andronova, F. Szydlo, F. Teply, M. Tobrmanova, A. Volot, I. G. Stara, I. Stary, L. Rulisek, D. Saman, J. Cvacka, P. Fiedler, P. Vojtisek, *Collect. Czech. Chem. C.* **2009**, *74*, 189–215; c) I. G. Stará, A. Andronova, A. Kollarovic, S. Vyskocil, S. Juge, G. C. Lloyd-Jones, P. J. Guiry, I. Stary, *Collect. Czech. Chem. Commun.* **2011**, *76*, 2005–2022.

[11] H. Kelgtermans, L. Dobrzanska, L. Van Meervelt, W. Dehaen, *Org. Lett.* **2012**, *14*, 1500–1503.

[12] D. Waghray, J. Zhang, J. Jacobs, W. Nulens, N. Basarić, L. Van Meervelt, W. Dehaen, *J. Org. Chem.* **2012**, *77*, 10176–10183.

[13] a) W. Van Rossom, W. Maes, L. Kishore, M. Ovaere, L. Van Meervelt, W. Dehaen, *Org. Lett.* **2008**, *10*, 585–588; b) V. Mamane, F. Louerat, J. Lehl, M. Abboud, Y. Fort, *Tetrahedron* **2008**, *64*, 10699–10705; c) K. S. Masters, T. R. M. Rauws, A. K. Yadav, W. A. Herrebout, B. Van der Veken, B. U. W. Maes, *Chem. Eur. J.* **2011**, *17*, 6315–6320.

[14] a) O. Meth-Cohn, B. Narine, B. Tarnowski, *Tetrahedron lett.* **1979**, *20*, 3111–3114; b) B. Baruah, P. J. Bhuyan, *Tetrahedron* **2009**, *65*, 7099–7104.

[15] W. Van Snick, W. Nulens, S. Jambons, W. Dehaen, *Synthesis* **2009**, 767–774.

[16] C. Bazzini, T. Caronna, F. Fontana, P. Macchi, A. Mele, I. Natali Sora, W. Panzeri, A. Sironi, *New J. Chem.* **2008**, *32*, 1710–1717.

[17] a) R. H. Martin, M. J. Marchant, *Tetrahedron* **1974**, *30*, 347–349; b) R. H. Janke, G. Haufe, E.-U. Würthwein, J. H. Borkent, *J. Am. Chem. Soc.* **1996**, *118*, 6031–6035.

[18] a) S. Abbate, C. Bazzini, T. Caronna, F. Fontana, F. Gangemi, F. Lebon, G. Longhi, *Inorg. Chim. Acta* **2007**, *360*, 908–912; b) M. B. Groen, H. Wynberg, *J. Am. Chem. Soc.* **1971**, *93*, 2968–2974.

[19] a) M. Miyasaka, M. Pink, A. Olankitwanit, S. Rajca, A. Rajca, *Org. Lett.* **2012**, *14*, 3076; b) Y. H. Tian, G. Park, M. Kertesz, *Chem. Mater.* **2008**, *20*, 3266; c) X. Guégano, A. L. Kanibolotsky, C. Blum, S. F. L. Mertens, S.-X. Liu, A. Neels, H. Hagemann, P. J. Skabara, S. Leutwyler, T. Wandlowski, A. Hauser, S. Decurtins, *Chem. Eur. J.* **2009**, *15*, 63–66; d) B. W. D'Andrade, S. Datta, S. R. Forrest, P. I. Djurovich, E. Polikarpov, M. E. Thompson, *Org. Electron.* **2005**, *6*, 11–20.

[20] M. Maus, E. Rousseau, M. Cotlet, G. Schweitzer, J. Hofkens, M. Van der Auweraer, F. C. De Schryver, *Rev. Sci. Instrum.* **2001**, *72*, 36.

[21] D. V. O'Connor, D. Phillips, *Time-correlated single photon counting*, Academic Press, London, Orlando, **1984**.

[22] SAINT, Manual Version 5/6.0, Bruker Analytical X-ray systems, Madison, WI, **1997**.

[23] a) SHELXTL-NT, Manual Version 5.1, Bruker Analytical X-ray Systems, Madison, Wisconsin, **1997**; b) G. M. Sheldrick, *Acta Crystallogr. Sect. A* **2008**, *64*, 112.

[24] A. L. Spek, *Acta Crystallogr. Sect. D* **2009**, *65*, 148.

Received: March 4, 2013
Published online: ■■ ■■, 0000

